*Advanced Materials Research* *Online: 2014-08-11*
*ISSN: 1662-8985, Vol. 996, pp 128-134*
*doi:10.4028/www.scientific.net/AMR.996.128*


# Residual Stress Tensor Distributions in Cracked Austenitic Stainless Steel Measured by Two-Dimensional X-ray Diffraction Method

Youichi Saito[1, 2, a], Shun-Ichiro Tanaka[b]

[1]Graduate School of Engineering, Tohoku University, 6-6-02 Aza-Aoba, Aramaki, Aoba-ku, Sendai 980-8579, Japan.

[2]Nippon Yakin Kogyo Co., Ltd., Technical Research Center, 4-2 Kojima-cho, Kawasaki-ku, Kawasaki 210-8558, Japan.

[3]Institute of Multidisciplinary Research for Advanced Materials, Tohoku University, 2-1-1 Katahira, Aoba-ku, Sendai 980-8577, Japan.

[a]youichi.saitou@nyk.jp, [b]sitanaka@tagen.tohoku.ac.jp

**Keywords**: X-ray diffraction method, austenitic stainless steel, continuous casting

**Abstract.** The residual stress tensor for cracked austenitic stainless steel was measured by a two-dimensional X-ray diffraction method. Higher von Mises equivalent stress concentrations, attributed to hot crack initiation, were obtained at both crack ends. The stress of 400 MPa at the crack end in the columnar grain region was about two-fold larger than that of 180 MPa in the equiaxed grain region. This difference was caused by a depression in the cast slab.

## Introduction

Stress and strain are inevitable in cast materials, and they can cause damage by hot crack initiation, owing to the thermal gradient in the material during solidification and cooling. In this study, we focus on hot cracks, which are defined as cracks initiated in the solid-liquid coexistence region, and include solidification, liquation, and ductility-dip cracks. In continuous casting of Fe- and Ni-based alloys, hot cracks should be prevented because they remain after rolling. A mechanism of crack and deformation generation in the solid-liquid coexistence region has been proposed. However, there has been little discussion of experimental stress values because it is difficult to measure stress and strain on a millimeter scale in cast alloys. If these measurements can be obtained, analysis can prevent the formation of hot cracks in cast alloys.

X-ray diffraction methods have been used to measure stress because they are nondestructive and precise. The conventional $\sin^2\psi$ method is widely used and has been improved over time. Tanaka and coworkers evaluated residual stress distributions for $Si_3N_4$ in a $Si_3N_4$/Cu/steel joint over a localized irradiation area of less than 0.03 $mm^2$[1,2]. If this method can be applied to cast alloys, the localized stress values will elucidate the initiation of cracks. However, measurements in cast alloys have been prevented by coarse and preferentially oriented grains. In this study, we used the two-dimensional X-ray diffraction method developed by He and Kingsley to measure the distribution of residual stress tensors, which entails irradiating the sample with multidirectional

X-rays to obtain diffraction patterns using a two-dimensional detector[3,4]. We optimized this method for measuring residual stress tensors in cast austenitic stainless steel to clarify the effect of crack initiation.

**Experimental**

**1. Specimen**

A Fe-20wt.%Ni-20wt.%Cr-Si-Mn-0.4wt.%Al-0.4wt.%Ti (UNS-S33400) alloy was cast using a continuous casting machine. The alloy is a heat resistant austenitic stainless steel with a solidus line temperature of 1370 °C. A specimen 120 × 40 × 15 mm (l × w × d) in size was cut from the shorter side of the slab at a speed of 1.5 mm/min using a cold working method (Fig. 1). The horizontal direction of the slab was defined as the x-axis, the vertical direction as the y-axis, and the casting direction as the z-axis. The measured plane was the cross section against the z-axis. The sample was chemical etched to eliminate surface strain. There were hot cracks initiated along the width (x-axis) of this plane during solidification. The length of the hot cracks was 50 mm. The plane consisted of a columnar and an equiaxed grain region. The maximum size of the columnar grains was 5 mm. However, each grains were consisted by a lot of dendrites which tilt at the range of a few degrees each other by observation of optical microscope.

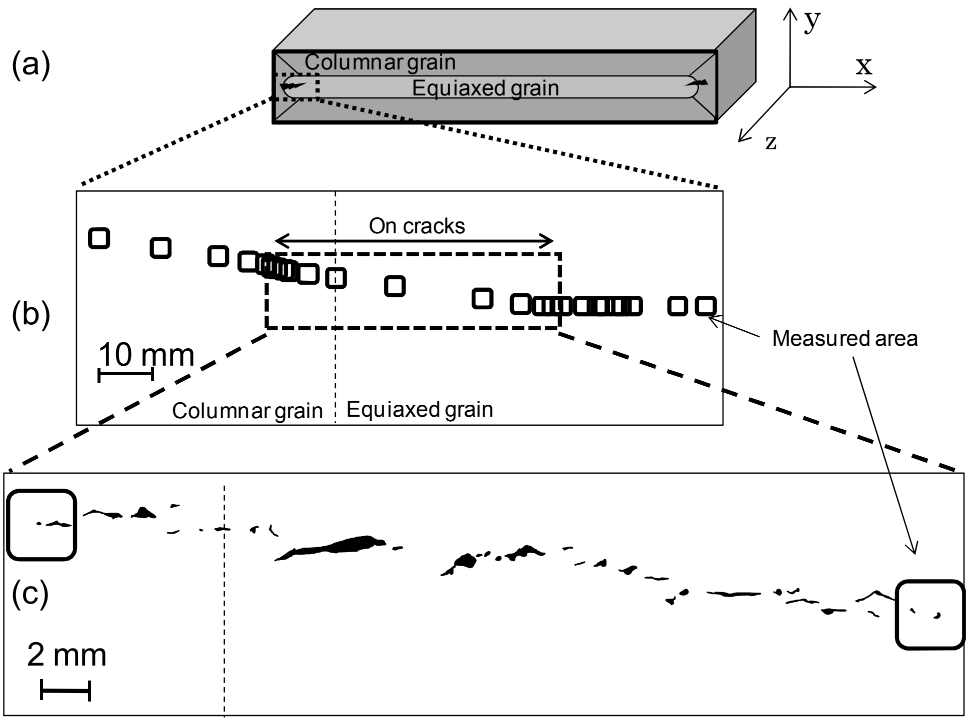


**Fig. 1.** Schematic of the specimen prepared from a continuously cast austenitic stainless steel slab. The cross section was taken against the casting direction. The enlargement shows the area around the cracks. The dotted square shows the measured area and the broken vertical line in the specimen shows the boundary between the columnar and equiaxed grains. The shape of the cracks is shown in (c), where the cracks were initiated intermittently.

## 2. Measurement of residual stress tensor

The conditions for stress tensor measurement by two-dimensional X-ray diffraction are shown in Table 1. The specimen was held on a stage and tilted an angle of $\psi$ along the cradle, and rotated by an angle of $\phi$ around the Cr-K$\alpha$ X-ray irradiation center. In addition, the specimen was oscillated by 1 mm along the x- and y-axes. These conditions were optimized to obtain a continuous Debye-Scherrer ring from a sufficient number of grains in an area of 9 mm$^2$. The X-rays penetrated the specimen to a depth of 5 $\mu$m in the measurement area. The X-rays were collimated to 1.0 mm in diameter and diffracted at $2\theta_0$ = 129°, which corresponds to the $\gamma$-austenite (220) plane according to previous X-ray diffraction results.

The measurement areas for residual stress tensor measurements are shown in Fig. 1. The residual stress tensor values were the average values for a 9 mm$^2$ area. The measurement points were around hot cracks. Many measurements were taken near the crack ends, because very precise values were required to assess the effect of hot cracks on the residual stress tensor distributions. Twenty-five combinations of specimen tilt angles along the $\omega$, $\psi$, and $\phi$ axes were used, and the measurement time for each combination was 90-1200 s, depending on how long it took obtain a continuous Debye-Scherrer ring. Residual stress tensor values were obtained by analyzing the shift, broadening and twist of the X-ray diffraction peak and shape of a Debye-Scherrer ring compared with that of the stress-free crystal lattice. Measured values might be different from the values predicted by peak shift of Debye-Scherrer ring simply. The results were analyzed with values of Young's modulus, the longitudinal elastic modulus, and Poisson's ratio as 197 and 74 GPa, and 0.33, respectively. These values were obtained by preparatory experiments. The normal, shear, principal, and von Mises equivalent stresses were calculated.

**Table 1.** Measurement conditions for the residual stress tensor of austenitic stainless steel by two-dimensional X-ray diffraction. The collimator size and oscillation range were optimized to obtain a continuous Debye-Scherrerring from a sufficient number of grains.

| | |
|---|---|
| X-ray type | Cr-K$\alpha$ |
| X-ray power | 38 kV-16 mA |
| Diffraction plane | $\gamma$-austenite |
| Diffraction angle | $2\theta_0$=129° |
| Measurement time | 90~1200 s/frame |
| Collimator size | $\phi$1.0 mm |
| Oscillation | ±1 mm |

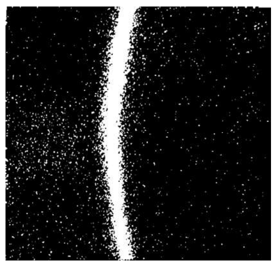


(a) Obtained Debye-Scherrer ring irradiated for 1200 s, oscillated for 1 mm

(b) Irradiation time: 90 s Oscillation range: 1 mm

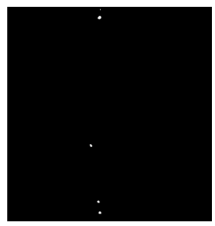

(c) Irradiation time: 90 s No oscillation

**Fig. 2.** Debye-Scherrer rings obtained from the two-dimensional detector. The diffraction angle was 132°, and the detected area was 117 to 147°. (a) shows the results for irradiation time of 1200 s, (b) shows results for an irradiation time of 90 s and (c) shows the results for an irradiation time of 90 s without oscillation of the specimen.

**Residual stress tensor distribution along hot cracks**

The measurement conditions where a continuous Debye-Scherrer ring was obtained are shown in Fig. 2. The curved line was set at $2\theta_0 = 129°$ and the detected diffraction angle range was from 114° to 144°. The Debye-Scheller ring obtained after 90 s irradiation shown in (b) was weaker compared with the Diffracted X-ray plot than the ring obtained after 1200 s shown in (a). The error range was reduced by increasing irradiation time. In contrast, if preferentially oriented grains occupied a large proportion of the measurement area and if the specimen was not oscillated during measurements, the ring would not have the shape shown in (c). The error in the residual tensor values would also be much higher for preferentially oriented grains and static measurements.

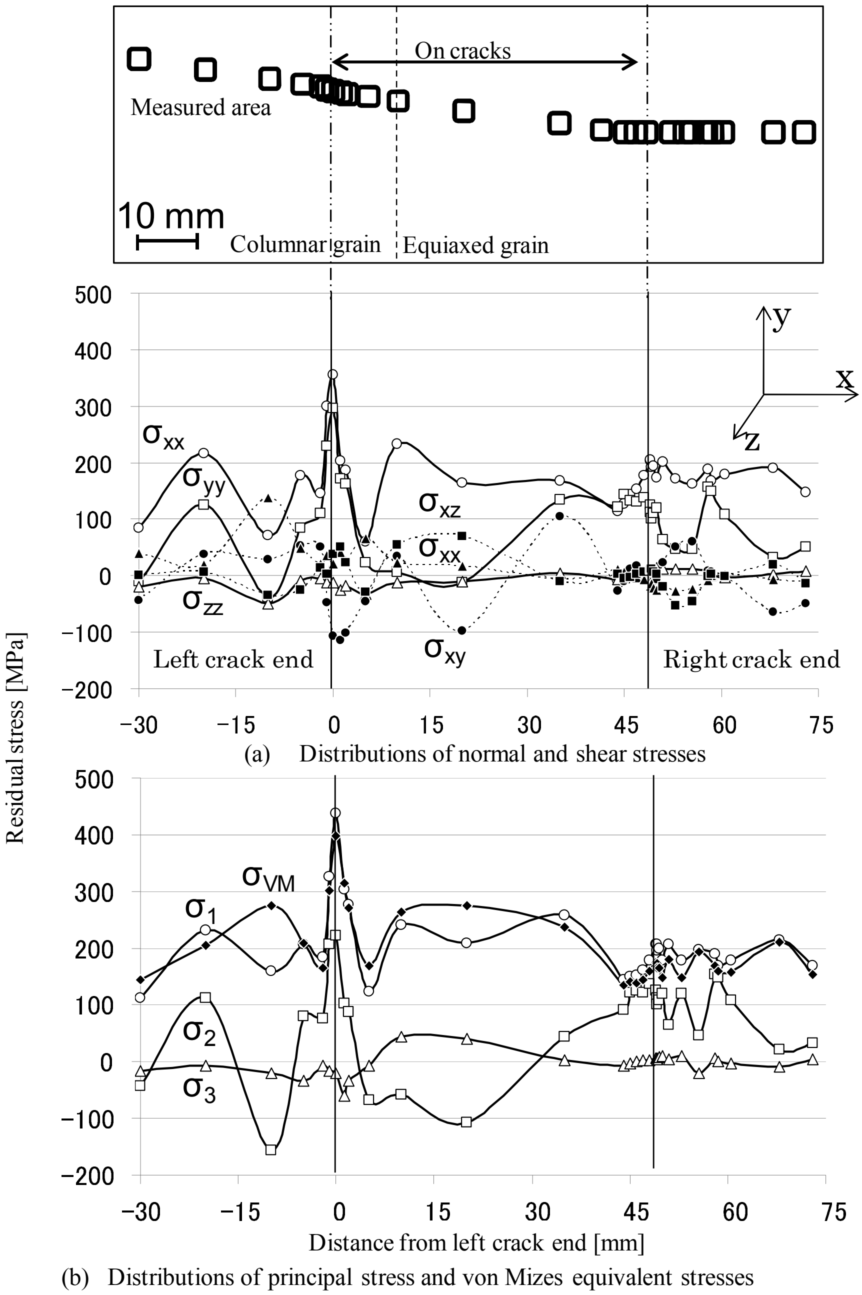


**Fig. 3.** Residual stress tensor distributions along hot cracks. (a) Normal and shear stress (b) Principal and von Mizes equivalent stress.

Figure 3 shows the residual stress tensor distribution along the direction of the hot cracks. The horizontal axis indicates the distance from the left crack end, and the vertical axis indicates the residual stress tensor values. Normal ($\sigma_{xx}$, $\sigma_{yy}$, $\sigma_{zz}$), shear ($\sigma_{xy}$, $\sigma_{yz}$, $\sigma_{xz}$), principal ($\sigma_1$, $\sigma_2$, $\sigma_3$), and equivalent ($\sigma_{VM}$) stress values are shown. The following results were obtained from the distribution.

Normal stresses along the horizontal direction of the slab, $\sigma_{xx}$, were higher than $\sigma_{yy}$ along the longitudinal direction of the slab at all measurement points and the error for the values was within 30 MPa. There were stress concentrations for $\sigma_{xx}$ and $\sigma_{yy}$ in a 5 $mm^2$ area at both crack ends. This indicates that stress may remain and initiate hot cracks. The normal stresses at the left crack end, where $\sigma_{xx}$ was 350 MPa and $\sigma_{yy}$ was 300 MPa, were higher than those at the right crack end, where $\sigma_{xx}$ was 200 MPa and $\sigma_{yy}$ was 100 MPa. $\sigma_{zz}$ along the casting direction of the slab was -50 to 15 MPa and the error for the values was within 15 MPa. Although these values had error range, it could be because the strain along the cast direction was lower and the specimen was under plane stress condition. Shear stresses $\sigma_{xy}$, $\sigma_{yz}$, and $\sigma_{zx}$ were within 100 MPa and the error for the values was within 20 MPa in all measured areas.

Principal stresses $\sigma_1$ and $\sigma_3$ showed the same behavior as $\sigma_{xx}$ and $\sigma_{zz}$. This was because the shear stresses were so low that $\sigma_1$ had a value similar to $\sigma_{xx}$, although they were higher than the normal stresses along other axes, thus the maximum principal stress also followed a similar trend. $\sigma_{zz}$ also followed this pattern. Although $\sigma_2$ showed a trend similar to $\sigma_{yy}$, the compressive stress values near the left crack end were -150 MPa, and fluctuated slightly from the right crack end to inner area of the slab. The von Mises equivalent stress, $\sigma_{VM,}$ was similar to $\sigma_1$, because $\sigma_2$ and $\sigma_3$ were lower than $\sigma_1$. The elastic strain of the specimen was affected mainly by the tensile stress along the x-axis. Local maximum values of 400 and 180 MPa were measured at the left and right crack ends, respectively.

**Difference between stress at left and right crack ends**

There are two possible hypotheses to explain difference between stress at left and right crack ends. The first is that the cracks propagated from one side to the other, and both sides showed a large relaxation or concentration of stresses. The second is that the degree of stress concentration was different depending on the grain size and shape during crack initiation and propagation. The first hypothesis is supported by the observation that the slab bulged on the long side and the formation

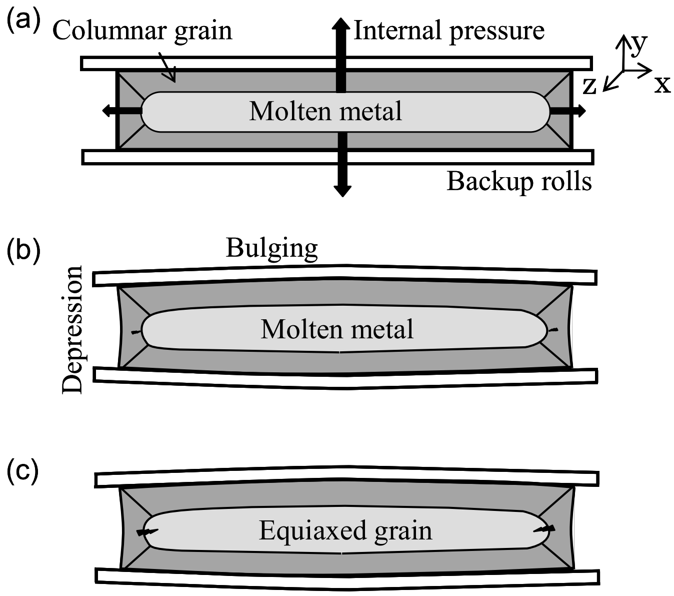


**Fig. 4.** Schematic of bulging to explain difference between stress at left and right crack ends. (a) Solidified shell is loaded with internal pressure from the molten metal. (b) Deformation is suppressed by the pinch force from the backup rolls which generates a depression on the shorter side of the slab. (c) The solidified shell is loaded with stress along the y direction and relaxed many times until solidification is completed.

of a millimeter-scale depression on the short side. This deformation is a well-known defect seen in continuously cast alloys as shown in Fig. 4. It is caused by the internal pressure of the molten metal, which remains in the cast slab until solidification is complete, and by the load applied by the support and pinch rolls in the machine. Internal pressure is also generated by gravity and pushes the alloy outwards; however, the set rolls suppress the deformation. The corner of the slabs cools more quickly than other side, which deforms some types of alloys. The left crack end was located near the shorter side of slab; the depression may add to the stress that causes crack initiation. In contrast, the larger stress values at the left crack end remained as stress concentrations when crack propagation was stopped. This suggests that the temperature gradient during solidification should be gradual to reduce deformation. It could be controlled by decreasing the amount of additional elements which increase the temperature range between the liquidus and solidus lines.

**Values of $\sigma_{xx}$ and $\sigma_{yy}$**

The higher values of $\sigma_{xx}$ than $\sigma_{yy}$ meant that the cast slab had a larger elastic strain along the x (horizontal) direction than along y (longitudinal) direction. This may be because of the following reasons.

1. Internal pressure causing the solidifying shell in the cast slab to bulge as mentioned above. The bulging of the cast slab deformed the specimen and could initiate hot cracks, while they decreased elastic strain along the longitudinal direction. After solidification, elastic/plastic stresses were generated by thermal shrinkage. If the stress was the same level along the x and y directions, the distribution remains when the deformation and crack initiation are at room temperature, and $\sigma_{xx}$ is higher than $\sigma_{yy.}$

2. Thermal shrinkage under restrained conditions along the long side of the slab

If the shape of the cast material is isotropic, thermal shrinkage occurs homogeneously in all directions. However, the specimen was cut from a cast slab with a long side 7.5-fold longer than the short side. Therefore, the thermal shrinkage was similar to that for a rod, and large internal tensile stresses were generated along the long direction of the slab.

3. Cutting and planing strain

Although the specimen was chemically etched to eliminate processing strain, some residual strain may have been present when the measurement was carried out. Cutting and planing were carried out along the x (horizontal) direction of the slab; therefore, $\sigma_{xx}$ possibly increased compared with the original stress and $\sigma_{yy}$ values.

**Conclusions**

(1) The residual stress tensor of a cast austenitic stainless steel alloy with a grain size of 1-5 mm was measured with an error of 30 MPa by two-dimensional X-ray diffraction method. In the case of cast alloys, columnar and eauiaxed grains were consisted by part of dendrites which tilt at the range of a few degrees.

(2) Local maximum values of the von Mises equivalent stress tensor were detected at the crack ends in the sample.

(3) The stress values at the left crack end were two-fold larger than those at the right crack end. This was caused by the deformation of the cast slab or differences in the stress concentration/relaxation depending on grain size or shape. To prevent cracks from initiating, the concentration of additional elements should be reduced to reduce the temperature difference between the liquidus and solidus line.

(4) $\sigma_{xx}$ was higher than $\sigma_{yy}$ because of the tensile stress caused by the bulging of the solidifying shell of the cast slab, thermal shrinkage under restrained conditions along long side of the slab, and cutting and planing strain during preparation.

**References**

[1] S.-I. Tanaka, Yumiko Takahashi: ISIJ International **30**(1990)12, 1086-1091

[2] K. Honda, S. Yokoyama, S.-I. Tanaka: Journal of applied physics **10**(85)7380

[3] Bob B. He: “Two-Dimensional X-Ray Diffraction” (2009) Wiley

[4] Bob B. He and Kingsley L. Smith, A New Method for Residual Stress Measurement Using an Area Detector, Proceedings of ICRS-5, Linkoping, Sweden, 1997.